J. Braz. Chem. Soc., Vol. 16, No. 1, 17-23, 2005.
Printed in Brazil - ©2005 Sociedade Brasileira de Química
0103 - 5053 $6.00+0.00

Article

Olefin Hydroformylation by Sol-gel Entrapped Rhodium Catalysts Bearing Hydrolysable Ligands

José Daniel Ribeiro de Campos and Regina Buffon*

Instituto de Química, Universidade Estadual de Campinas, CP 6154, 13084-971 Campinas - SP, Brazil

Complexos de ródio preparados *in situ* a partir de $[Rh(OMe)(COD)]_2$, $[Rh(CO)_2(acac)]$, [Rh(cod)(acac)] ou $[Rh(cod)(PPh_3)_2]^+BPh_4^-$ com ligantes como $HS(CH_2)_3Si(OMe)_3$, $Ph_2P(CH_2)_2S(CH_2)_3Si(OMe)_3$ ou $Ph_2P(CH_2)_2Si(OMe)_3$ foram imobilizados em matrizes de sílica, inorgânicas ou híbridas, pelo processo sol-gel. As matrizes inorgânicas foram preparadas apenas com tetrametilortossilicato enquanto que para as híbridas foram utilizados 1,4-*bis*(trietoxissilil)benzeno ou 1,2-*bis*(trietoxissilil)etano como agentes de co-condensação. O sistema baseado em $[Rh(CO)_2(acac)]$/ $Ph_2P(CH_2)_2S(CH_2)_3Si(OMe)_3$ foi ativo na hidroformilação de 1-hexeno e de 1-octadeceno sem lixiviação de ródio. Também pôde ser usado na ausência de solvente, como observado na hidroformilação do 1-deceno. Apesar do melhor sistema obtido apresentar uma matriz microporosa, não foi possível estabelecer uma correlação direta entre composição da matriz, grau de condensação da mesma e propriedades da superfície.

Rhodium complexes prepared in situ from $[Rh(OMe)(COD)]_2$, $[Rh(CO)_2(acac)]$, [Rh(cod)(acac)] or $[Rh(cod)(PPh_3)_2]^+BPh_4^-$ with ligands as $HS(CH_2)_3Si(OMe)_3$, $Ph_2P(CH_2)_2S(CH_2)_3Si(OMe)_3$ or $Ph_2P(CH_2)_2Si(OMe)_3$ were immobilized in inorganic and hybrid silica matrices *via* the sol-gel process. The inorganic matrices were prepared with tetramethylorthosilicate while for the hybrid ones 1,4-*bis*(triethoxysilyl)benzene or 1,2-*bis*(triethoxysilyl)ethane were used as co-condensation agents. The system based on $[Rh(CO)_2(acac)]$/ $Ph_2P(CH_2)_2S(CH_2)_3Si(OMe)_3$ was active in the hydroformylation of 1-hexene and 1-octadecene without any rhodium leaching. It could also be used in the absence of a solvent, as observed in the hydroformylation of 1-decene. Although the best system was based on a hybrid microporous matrix, no straightforward correlation between matrix composition, condensation degree and surface properties could be found.

Keywords: sol-gel process, hydroformylation, rhodium

Introduction

Hydroformylation of olefins is the largest scale homogeneous catalytic reaction.[1] Homogeneous catalysis, however, presents several drawbacks, in particular the recovering of the catalyst at the end of the process, warranting a search for two-phase or immobilized catalysts. In the last years, the sol-gel method has been applied as an alternative to immobilize soluble catalysts, using either inorganic[2] or hybrid[3] matrices. Recently, we reported the use of this approach to prepare rhenium-, molybdenum- and vanadium-based epoxidation catalysts,[4-6] as well as ruthenium- and rhodium-based catalysts for the hydrogenation and hydroformylation of olefins, respectively.[7,8] Depending on the characteristics of the matrix, leaching-free systems could be prepared even when the transition metal complex was just physically entrapped inside the porous system. In the case of rhodium complexes containing a diphosphine and no ligand bearing a hydrolysable group, only a microporous matrix would lead to recyclable catalysts.[8] An interesting and robust rhodium catalyst system containing a xanthene-based hydrolysable ligand was previously described,[9] but the matrix was not characterized. We wish to report here some results concerning the immobilization of rhodium complexes in silica matrices prepared by the sol-gel method using ligands bearing hydrolysable groups and their use in the hydroformylation of olefins.

Experimental

Complexes $[Rh(OMe)(cod)]_2$,[10] [Rh(cod)(acac)],[11] $[Rh(cod)(PPh_3)_2]^+BPh_4^-$;[12] ligands $Ph_2P(CH_2)_2Si(OMe)_3$,[13] $Ph_2P(CH_2)_2S(CH_2)_3Si(OMe)_3$,[14] and the co-condensation

* e-mail: rbuffon@iqm.unicamp.br

agent 1,4-*bis*(triethoxysilyl)benzene[15] were prepared according to the literature. The co-condensation agent 1,2-*bis*(triethoxysilyl)ethane was prepared by metathesis of (triethoxysilyl)vinyl (Aldrich) followed by hydrogenation. $[Rh(CO)_2(acac)]$ and XANTPHOS were purchased from Strem Chemicals; $HS(CH_2)_3Si(OMe)_3$, from Aldrich. THF (Merck) was dried over Na/benzophenone just before use.

Catalyst preparation

In a typical preparation, 5 mg (~10 mmol) of the rhodium precursor and a corresponding equivalent of the ligand ([P]:[Rh]=2:1) were added to a 50 mL Schlenk flask containing 6 mL of THF. The solution was kept under stirring for 15 min, followed by the addition of 2 mL (11.10 mmol) of deionized water, 2 mL (13.56 mmol) of TMOS (tetramethylorthosilicate), 1 mL (~3.4 mmol) of the co-condensation agent (in the case of hybrid matrices), methanol (*ca.* 1 mL, amount needed to obtain a clean solution) and 4 drops of a 3wt.% solution of $(AcO)_2Sn(Bu)_2$ in polydimethylsiloxane (Dow Corning). The solution was stirred for 15 min and allowed to stand until gelation (from one night to 8 days, depending on the case). The gel thus obtained was dried under vacuum, washed with CH_2Cl_2 in a Soxhlet and dried again under vacuum at room temperature. The resulting yellow-orange materials were stored under air at room temperature.

Catalytic experiments

All catalytic experiments were performed in a 100 mL stainless steel Parr reactor. The reaction temperature was kept at 80 °C and the solution was stirred at 300 rpm. In a typical experiment, 2-5 μmol of the rhodium complex (~250 mg of the catalyst), 0.28 g (2-5 mmol) of 1-hexene ([Rh]/[olefin] ~1/1000), 0.1 g of cyclooctane (internal standard) and 30 mL of THF (solvent) were employed. The reactor was first purged with H_2, and then pressurized at 50 bar (CO/H_2 = 1/1). For recycling experiments, the catalyst was separated by filtration, washed in a Soxhlet with CH_2Cl_2, dried under vacuum and used in a new run. All procedures were performed under air. GC analyses were carried out in an HP5890 series II gas chromatograph, equipped with an HP5 capillary column (50 m x 0.2 mm) and a flame ionization detector. Products were quantified using calibration curves obtained with standard solutions.

Catalyst characterization

Nitrogen adsorption isotherms were determined at -196 °C with a Micromeritics ASAP 2010 automated porosimeter. All calculations were performed using the associated Micromeritics software. Samples were degassed at 80 °C for a minimum of 24 h prior to measurements.

Rhodium concentrations were determined through ICP-AES analyses (Perkin-Elmer Optima 3000 DV).

TEM images were obtained on a Zeiss CEM-902 apparatus equipped with a CCD-Proscan camera and a high speed/slow scan system controller. The samples were suspended in *iso*-propanol and dispersed on carbon-coated copper grids.

^{29}Si MAS NMR spectra were recorded on a Bruker AC 300 spectrometer using zirconia rotors and the following conditions: delay between each scan = 15 s; acquisition time = 0.1 s. Typically, 5 000 scans were accumulated. Solution ^{31}P NMR spectra were recorded on a Gemini 300 P instrument at 121.5 MHz, in $CDCl_3$.

Results and Discussion

In order to determine the effects of the nature of the rhodium complex on the properties of the resulting matrix, four different precursors, *viz.* $[Rh(OMe)(cod)]_2$, [Rh(cod)(acac)], $[Rh(CO)_2(acac)]$ and $[Rh(cod)(PPh_3)_2]^+BPh_4^-$, as well as three ligands bearing hydrolysable groups, *viz.* $HS(CH_2)_3Si(OMe)_3$, $Ph_2P(CH_2)_2Si(OMe)_3$ and $Ph_2P(CH_2)_2S(CH_2)_3Si(OMe)_3$ were employed. The acac-containing complexes were expected to lead to mesoporous matrices, which would facilitate diffusion of the substrates.[8] The ligand $HS(CH_2)_3Si(OMe)_3$ would lead to a dimer whose anchoring to silica has been reported to give an almost leachless system.[16] Two co-condensation agents were also tested, 1,4-*bis*(triethoxysilyl)benzene and 1,2-*bis*(triethoxysilyl)ethane, aiming to reduce the degree of 3D-cross-linking, decreasing the rigidity and improving the swelling properties of the resulting matrices. The expected immobilized rhodium species are depicted in Scheme 1. The structures of systems **I+XANTPHOS**, and **III**, **IV** are proposed on the basis of their ^{31}P NMR spectra obtained before gelation. For systems **II** and **III**, the free $acac^-$ ligand would deprotonate a silanol group form the surface, producing a $\equiv SiO^-$ anion.[9] The same anion could be formed in system **IV** *via* a reaction between BPh_4^- and a silanol group. It must be kept in mind, however, that the ionic species depicted in Scheme 1 would be present only in a fresh catalyst: under hydroformylation conditions, the cationic species are neutralized[17] and systems **II** to **IV** would eventually be of the type $[RhH(CO)_xL_2]$, where L = is a neutral ligand bearing P or S as donor atoms.

Systems based on inorganic matrices are labeled with the index **a**; **b** and **c** are related to hybrid matrices based on 1,4-*bis*(triethoxysilyl)benzene and 1,2-*bis*(triethoxysilyl)ethane, respectively. All systems were

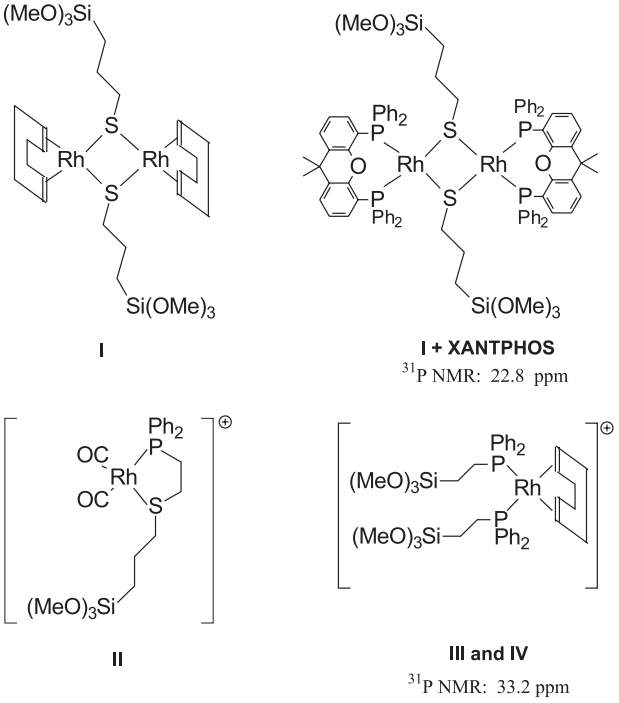

Scheme 1.

characterized by ^{29}Si MAS NMR and, whenever possible, also by nitrogen adsorption/desorption isotherms.

Catalyst characterization

The nitrogen adsorption/desorption isotherms of catalysts **Ia**, **IIb** and **IIIa** are of type I (IUPAC classification),[18] typical of microporous systems (Figure 1). A small hysteresis is clearly observed only for catalyst **IIb**, suggesting that the pores are mainly smooth and cylindrical, with a low contribution of mesopores.[19] The Horvath-Kawazoe differential pore volume plots for these catalysts are shown in Figure 2. Catalyst **IVa** is characterized by a type IV isotherm (mesoporous) with a small contribution of micropores: the volume adsorbed at the lowest relative pressure represents ~20% of the total pore volume (Figure 1). Its BJH adsorption pore size distribution is shown in Figure 2. BET surface areas, pore volumes and average pore size determined from the isotherms, along with the final rhodium loading, are presented in Table 1. The amount of immobilized rhodium was always smaller than the added one, with the excess being washed away during Soxhlet extractions, which were repeated until a clean solution was obtained.

We failed to obtain isotherms for catalysts **Ib** and **Ic**. They were, therefore, characterized by transmission electron microscopy. Taking into account that these materials were able to entrap a relatively large amount of rhodium without leaching in the catalytic experiments (*vide infra*), their TEM micrographs, shown in Figure 3, suggest a dense structure with packed microporous domains.

^{29}MAS Si NMR spectra could provide a relationship between the condensation degree of TMOS and the porosity of the corresponding material. Figure 4 shows the spectra obtained for three different samples: an inorganic matrix (catalyst **Ia**); a hybrid matrix containing 1,4-

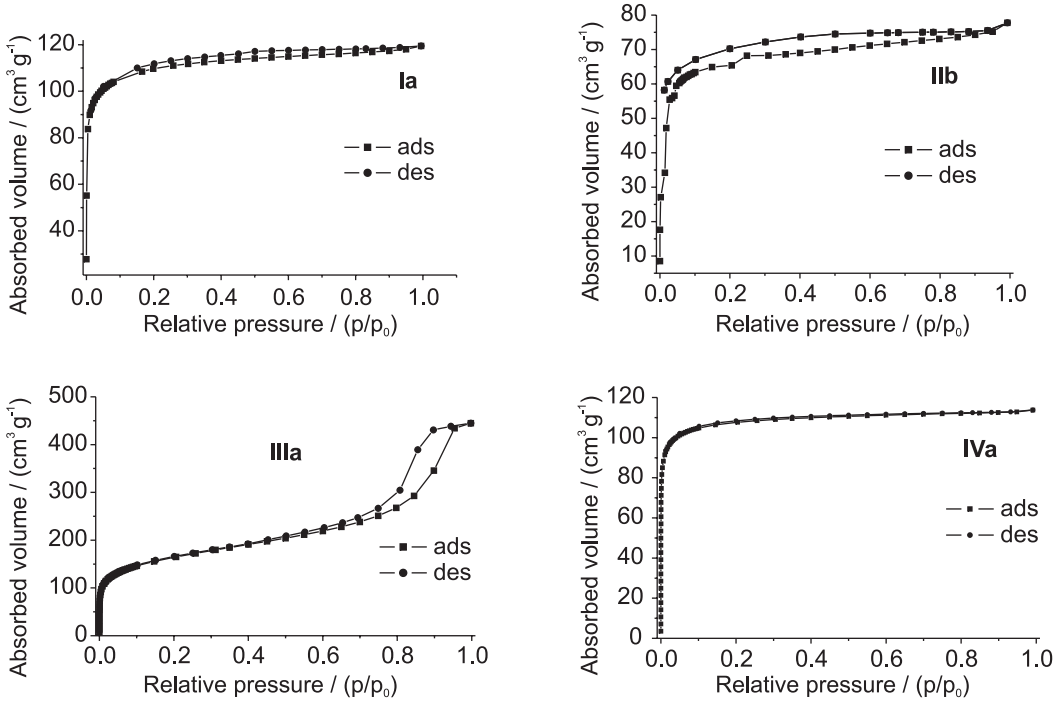

Figure 1. Nitrogen adsorption/desorption isotherms for some systems.

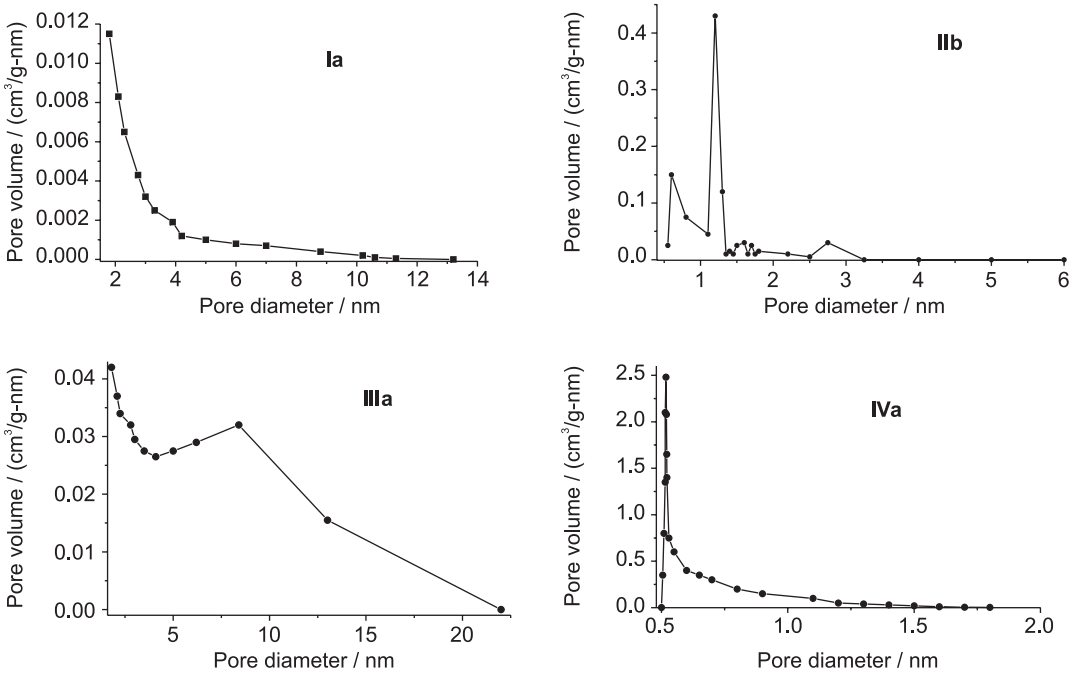

Figure 2. Pore size distribution for some systems.

Table 1. Composition and surface characteristics of the catalysts

System	Complex	Ligand[a]	Co-condensation Agent	Rh wt.%	Area BET m^2g^{-1}	Pore diameternm	Pore volume cm^3g^{-1}
Ia	$[Rh(OMe)(cod)]_2$	Si-SH	-	0.35	340	3.55[b]	0.18[b]
Ia + X	$[Rh(OMe)(cod)]_2$	Si-SH + XANTPHOS	-	0.31			
Ib	$[Rh(OMe)(cod)]_2$	Si-SH	$(EtO)_3SiPhSi(OEt)_3$	0.22			
Ib + X	$[Rh(OMe)(cod)]_2$	Si-SH + XANTPHOS	$(EtO)_3SiPhSi(OEt)_3$	0.17			
Ic	$[Rh(OMe)(cod)]_2$	Si-SH	$(EtO)_3Si(CH_2)_2Si(OEt)_3$	0.15			
IIb	$[Rh(CO)_2(acac)]$	Si-PS	$(EtO)_3SiPhSi(OEt)_3$	0.24	250	1.11[b]	0.12[b]
IIIa	[Rh(cod)(acac)]	$Si\text{-}PPh_2$	-	0.09	600	6.65[c]	0.69[c]
IVa	$[Rh(cod)(PPh_3)_2]^+$	$Si\text{-}PPh_2$	-	0.02	400	0.64[b]	0.18[b]

[a] Si-SH = $HS(CH_2)_3Si(OMe)_3$; Si-PS = $Ph_2P(CH_2)_2S(CH_2)_3Si(OMe)_3$; $Si\text{-}PPh_2$ = $Ph_2P(CH_2)_2Si(OMe)_3$; [b]Horvath-Kawazoe method; [c] BJH method.

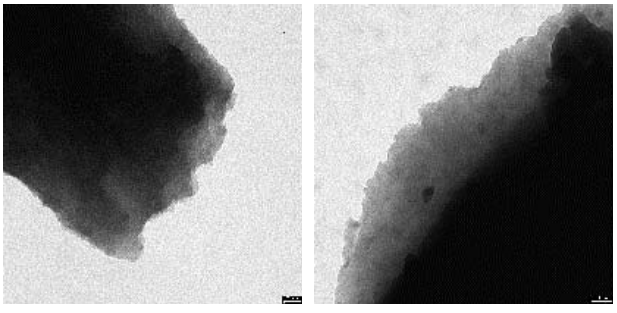

Figure 3. TEM micrographs for systems **Ib** (left) and **Ic** (right).

bis(triethoxysilyl)benzene (**IIb**) and a hybrid matrix based on 1,2-*bis*(triethoxysilyl)ethane (**Ic**). Table 2 shows the concentration of each type of silicon site: Q^2 [=$Si(OH)_2$, δ ~ -91]; Q^3 [≡Si(OH), δ ~ -101]; Q^4 [≡Si-O-Si≡, δ ~ -109]; T^1 [-$Si(OR)_2R'$, δ ~ -62 for systems **b**; ~ -45 for system **c**]; T^2 [=Si(OR)R', δ ~ -71 for systems **b**; ~ -53 for system **c**]

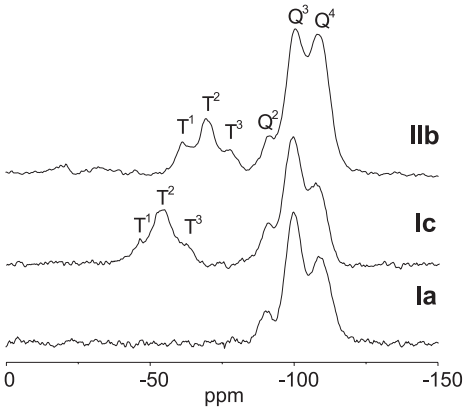

Figure 4. Characteristic ^{29}Si MAS NMR spectra.

and T^3 [≡Si-R', δ ~ -79 for systems **b**; ~ -63 for system **c**]. Signals corresponding to silicon atoms from the ligands could never be observed, probably due to the very low

Table 2. Concentration of silicon sites as obtained by ^{29}Si MAS NMR

Sample	T^1	T^2	T^3	Q^2	Q^3	Q^4	T^2/T^1	Q^4/Q^3	Q^4/Q^2
Ia	-	-	-	3.4	58.1	38.5	-	0.66	11.3
Ia + XANTPHOS	-	-	-	13.4	55.0	31.6	-	0.57	2.4
Ib	13.2	12.6	4.3	5.8	36.8	27.4	0.95	0.74	4.7
Ib + XANTPHOS	4.6	17.4	5.3	5.4	36.3	31.0	3.8	0.85	5.7
Ic	0.8	25.1	3.7	2.6	42.6	25.3	31.4	0.59	9.7
IIb	5.0	14.0	1.9	1.7	39.4	38.0	2.8	0.96	22.4
IIIa	-	-	-	7.8	39.5	52.6	-	1.33	6.7
IVa	-	-	-	5.5	40.9	53.6	-	1.31	9.7

concentration of such ligands relatively to TMOS (molar ratios: 1:1400 for system **IIb**; 1:700 for systems **I, III** and **IV**). Taking into account that the molar ratio [TMOS]/[co-condensation agent] was kept constant (=4) in all preparations, a $\Sigma Q^i/\Sigma T^i \sim 2/1$ was expected. However, such ratios varied from 2.3 (**Ib**) to 3.8 (**IIb**), suggesting that some amount of co-condensation agent was not incorporated into the matrix and was washed away during the Soxhlet treatment.

Comparing the Q^4/Q^3 ratio for systems **I**, the addition of a co-condensation agent appears to have little effect on the condensation degree of TMOS. The Q^4/Q^2 ratio, however, is strongly affected, with a high increase in the relative concentration of Q^2 sites, in particular for system **Ib**. For the hybrid matrices, T^2 sites predominate in the case of systems **Ic** and **IIb**; system **Ib**, however, presents a T^2/T^1 ratio close to one. T^3 sites are always minority. These results show that the overall 3D-cross-linking degree is indeed strongly affected by the addition of a co-condensation agent, but not always to the same extent. The highest degree of TMOS condensation is observed for systems **IIIa** and **IVa**, the only ones presenting Q^4/Q^3 ratios higher than 1.

Nevertheless, neither the condensation degree of TMOS nor the presence of a co-condensation agent can be directly correlated with surface area, pore diameter or pore volume. It seems that the nature of the rhodium complex plays an important role in determining the final characteristics of the matrix. Evidences are the changes in Q^4/Q^2 and T^2/T^1 ratios when system **Ia** and **Ib**, respectively, were prepared in presence of the ligand XANTPHOS (Table 2). On the other hand, in a previous work[8] it was observed that neutral rhodium complexes bearing an $acac^-$ ligand, or even cationic rhodium complexes always led to mesoporous matrices. It should be noted, however, the absence of a hydrolysable ligand in those systems. Therefore, the microporosity observed for systems **IIb** and **IVa** was a little surprising. Also surprising were the results obtained for systems **IIIa** and **IVa**: upon reaction between the precursor complex and the ligand, the same species should be immobilized (Scheme 1) but the matrices are strongly different. This result clearly implies that the nature of the free ligand plays an important role in determining the final characteristics of the matrix. The only similarity was the very small amount of entrapped rhodium species. Whether this fact is related to the high condensation degree of TMOS or to a possible cleavage of the hydrolysable ligand cannot be decided yet. However, a high condensation degree might force the hydrolysable ligand to the outside surface, which could account for the high leaching of rhodium in the absence of a chelating ligand.

Catalytic activity

All systems were tested in the hydroformylation of 1-hexene and the results are shown in Table 3. PPh_3 ($[PPh_3]/[Rh] = 5/1$) was added to systems **I** since the precursor complex is not active in hydroformylation.[20] When analyzing systems **I**, the importance of the matrix composition is clear as the catalyst based on the inorganic matrix (**Ia**) did not present any activity; for a hybrid matrix based on 1,2-*bis*(triethoxysilyl)ethane (**Ic**) the activity was very low but the system prepared with the co-condensation agent *bis*(triethoxysilyl)benzene (**Ib**) presented a reasonable activity and could be used in at least three runs without any rhodium leaching. The lack of activity observed for system **Ia** might be due to a non-interaction between the rhodium complex and the added PPh_3. Therefore, a new gel was prepared by addition of the chelating ligand XANTPHOS ($[XANTPHOS]/[Rh] = 2/1$) to the initial solution containing $[Rh(OMe)(cod)]_2$ and $HS(CH_2)_3Si(OMe)_3$. For comparison, a sample of system **Ib** was prepared in the same way. Both systems were active although the observed n/i ratios (ratio between normal and branched aldehydes) were rather lower than those reported for monomeric rhodium catalysts containing the ligand XANTPHOS ($n/i > 50$).[21]

Although system **IVa** presented the highest n/i ratio observed in this work, its catalytic activity was very low. This may be due to mass transfer limitations arising from a very

Table 3. Catalytic performance in the hydroformylation of 1-hexene[a]

System	Rh wt.%	Run	Conv.%[b]	n/i[c]	H/I[d]	TON[e]	Rh leaching
Ia[f]	0.35	1	0	-	-	0	no
Ia + X	0.31	1	22	1.9	1.1	220	no
Ib[f]	0.22	1	44	1.9	1.5	440	no
		2	30	1.8	1.1	300	no
		3	30	2.1	1.1	300	no
Ib + X	0.17	1	38	2.0	1.7	380	no
Ic[f]	0.15	1	3	1.2	0.7	30	no
Iib	0.24	1	57	2.0	1.6	570	no
		2	51	1.8	1.5	510	no
		3	25	1.9	1.3	250	no
		4	18	2.0	1.4	180	no
IIIa	0.09	1	91	1.0	1.5	910	high
Iva	0.02	1	7.4	2.5	-	74	no

[a] Reaction conditions: [Rh]/[olefin]=1/1000; 50 bar ([CO]/[H_2]=1/1); 80°C; 24 h; solvent: THF; [b] conversion to hydroformylation products; [c] ratio between normal and branched aldehydes; [d] ratio between hydroformylation and isomerization products; [e] TON = mol of aldehydes per mol of rhodium sites; [f] PPh_3 added to the reaction mixture ([PPh_3]/[Rh] = 5/1); X = XANTPHOS.

small pore diameter of the matrix (Figure 2). In contrast, the activity of system **IIIa** was due to leached rhodium, not retained by a matrix characterized by a large distribution of mesopores (Figure 2). System **IIb** turned out to be more active than all other systems prepared in this work. It was active in at least four runs, with a total TON of 1510, albeit some deactivation from run to run. When tested in the hydroformylation of 1-decene in the absence of a solvent ([Rh]/[olefin] = 1/4540), a TON of 2450 was observed after 24h (n/i = 1.5; H/I = 2.7). It was also active in the hydroformylation of 1-octadecene: using the same conditions employed for 1-hexene, a TON = 530 was obtained (close to the 570 value observed for 1-hexene in the first run, Table 3), with n/i = 2.3 and H/I = 1.7. Thus, in spite of a microporous matrix, higher linear substrates could be hydroformylated. Taking into account that a chelating hydrolysable ligand was employed, the location of the rhodium complex (inside the porous system or on the external surface of the matrix) is a question that could be raised. Therefore, system **IIb** was tested in the hydroformylation of limonene, a voluminous substrate (volume ~0,435 nm^3).[22] Within 24h no reaction was observed. In the same experimental conditions, with the system $[RhCl(CO)_2]_2$/BINAP in solution a 21% conversion to hydroformylation products was obtained in 4h. These results strongly suggest that the complex is indeed inside the porous system of the matrix and that the deactivation observed in successive runs is due to a degradation of the complex upon manipulation after each reaction (always performed under air).

Conclusions

Although it seems that the nature of the rhodium complex plays an important role in determining the final characteristics of the matrix, no direct correlation between rhodium complex, matrix composition, condensation degree and surface properties could be found. Therefore, a straightforward way to prepare a desired matrix with any metal complex remains to be found. The system based on $[Rh(CO)_2(acac)]$/ $Ph_2P(CH_2)_2S(CH_2)_3Si(OMe)_3$ was active in the hydroformylation of 1-decene in the absence of a solvent, without any rhodium leaching. In spite of its microporous matrix, this catalyst was also active in the hydroformylation of 1-octadecene. The lack of any activity in the hydroformylation of limonene suggests that the complex is indeed entrapped inside the porous system of the matrix.

Acknowledgements

Financial support from FAPESP, as well as a fellowship to J.D.R.C., are gratefully acknowledged.

References

1. Cornils, B.; Herrmann, W.A.; *Applied Homogeneous Catalysis with Organometallic Compounds*, VCH: New York, Vol. 1, 1996.
2. Blum, J.; Avnir, D.; Schumann, H.; *Chemtech* **1999,** *29*, 32.
3. Lindner, E.; Schneller, T.; Auer, F.; Mayer, H.A.; *Angew. Chem. Int. Ed.* **1999** *38*, 2155.
4. Dallmann, K.; Buffon, R.; *Catal. Commun.* **2000** *1,* 9.
5. Teixeira, S.; Dallmann, K.; Schuchardt, U.; Buffon, R.; *J. Mol. Catal. A: Chem.* **2002**, *182-183,* 167.
6. Pellegrino, R.B.; Buffon, R.; *J. Braz. Chem. Soc*. **2004**, *15*, 527.
7. Dallmann, K.; Buffon, R.; *J. Mol. Catal. A: Chem.* **2002***, 185*, 187.

8. Campos, J.D.R.; Buffon, R.; *New J. Chem.* **2003**, *27,* 446.
9. Sanden, A.J.; van der Veen, L.A.; Reek, J.N.H.; Kamer, P.C.J.; Lutz, M.; Spek, A.L.; van Leeuwen, P.W.N.M.; *Angew. Chem. Int. Ed.* **1999**, *38,* 3231.
10. Uson, R.; Oro, L.A.; Cabeza, J.A.; *Inorg. Synth.* **1985**, *23*, 127.
11. Cramer, R.; *J. Am. Chem. Soc.* **1964**, *86*, 217.
12. Schrock, R.R.; Osborn, J.A.; *J. Am. Chem. Soc.* **1971**, *93*, 2397.
13. Niebergall, V.W.; *Makromol. Chem.* **1962**, *52*, 218.
14. Capka, M.; Czakoová, M.; Hillerová, E.; Paetzold, E.; Oehme, G.; *J. Mol. Catal. A: Chem.* **1995**, *104*, L123.
15. Loy, D.A.; Jamison, G.M.; Baugher, B.M.; Myers, S.A.; Assink, R.A.; Shea, K.J.; *Chem. Mater.* **1996**, *8*, 656.
16. Gao, H.; Angelici, R.J.; *Organometallics* **1998**, *17*, 3063.
17. Pàmies, O.; Net, G.; Widhalm, M.; Ruiz, A.; Claver, A.; *J. Organomet. Chem.* **1999**, *587*, 136.
18. Sing, K.S.W.; Everett, D.H.; Haul, R.A.; Moscou, L.; Pierotti, R.A.; Rouquerol, J.; Siemieniewska, T.; *Pure Appl. Chem.* **1985**, *57*, 603.
19. Brinker, C.J.; Scherer, G.W.; *Sol-Gel Science: The Physics and Chemistry of Sol-Gel Processing*, Academic Press: San Diego, 1990, pp 522-525.
20. Angelici, R.J.; Gao, H.; *J. Mol. Catal. A: Chem.* **1999**, *145*, 83.
21. Kranenburg, M.; van der Burgt, Y.E.M.; Kamer, P.C.J.; van Leeuwen, P.W.N.M.; *Organometallics* **1995**, *14*, 3081.
22. Calculated using *GAUSSIAN 1998* (Revision A.9) computational programs from HF optimized geometries.

Received: April 27, 2004
Published on the web: November 12, 2004

FAPESP helped in meeting the publication costs of this article.